TRACKING SPACE DEBRIS USING RADAR OBSERVATIONS CAMPAIGNS HELD IN JULY AND AUGUST 2024

L. Macotela(1), T. Grydeland(1), D. Kastinen(2), I. Arntzen(1), J. Markkanen(3), A. Horstmann(4), D. J. Trosten(1), S. N. Anfinsen(1), J. Kero(2)

(1) NORCE Norwegian Research Centre, Tromsø, Norway
(2) Swedish Institute of Space Physics, Kiruna, Sweden
(3) EISCAT Scientific Association, Sodankylä, Finland
(4) ESA/ESOC - European Space Operations Centre, Darmstadt, Germany

ABSTRACT

Significant sources of space debris include derelict payloads and rocket bodies, explosion- and collision-fragments of satellites and other space-borne objects. In 2024, a notable debris-generating event occurred when the Long March 6A rocket broke apart shortly after launch, creating a cloud of debris in orbit. Due to its potential impact on orbital safety, this event quickly became a priority for monitoring. Additionally, since 2019, the rapid expansion of the Starlink constellation has added a large number of satellites to low Earth orbit, making it a critical focus for space object tracking.

This study utilizes monostatic beam-park observations collected by the European Incoherent Scatter Scientific Association (EISCAT) Ultra High Frequency (UHF) radar during July and August 2024 to analyse the populations associated with these two groups of space objects. A correlation analysis was performed by comparing radar measurements with a publicly available Two-Line Element (TLE) catalogue, allowing for the identification of radar detections linked to catalogued objects. Uncatalogued detections found near the Long March 6A object are likely fragments resulting from its breakup. Furthermore, a comparison of catalogued detections from 2024 to those from 2021 reveals an increase in Starlink satellite observations.

To further validate these findings, a cross-comparison analysis is conducted, using radar detections alongside simulated detections obtained from the Program for Radar and Optical Observation Forecasting (PROOF) software using the most recent available calibrated Meteoroid and Space Debris Terrestrial Environment Reference (MASTER) model population. Here, we also examine the consistency and accuracy of the experimental and simulated detections.

1 INTRODUCTION

Human activities in space have inadvertently resulted in the accumulation of a vast population of objects that no longer serve any functional purpose, collectively known as space debris. These range from defunct satellites, such as the Environmental Satellite (ENVISAT) [1], and abandoned rocket stages to fragments generated by explosions, collisions, and other destructive events. Additionally, smaller objects, including detached components, slag particles from solid-fuel rockets, and even flecks of paint, contribute to this growing issue. Major sources of space debris include derelict payloads, rocket bodies, and fragments resulting from satellite explosions and collisions. Currently, it is estimated that approximately 1 million objects larger than 1 cm are in orbit [2-4].

The growing population of space debris presents a significant threat to active satellites and space missions [5-8], as well as to infrastructure and human life on Earth's surface [9]. Consequently, tracking, understanding, and modelling the debris population and fragmentation events are essential for ensuring the sustainability of space operations. By doing so, active satellites and other critical infrastructure can be protected, potential collisions can be avoided, and the exponential growth of space debris can be mitigated [10].

Radar systems play a crucial role in space debris monitoring by penetrating beyond Earth's ionosphere, enabling transmitted radio waves to scatter off Resident Space Objects (RSOs) and produce detectable echoes. These echoes can be coherently integrated to determine key parameters, including range, range rate, and Radar Cross Section (RCS) [11]. Among the most effective methods for characterizing the RSO population are monostatic radar measurements with a fixed antenna beam direction, known as beam-park observations [12-14]. This technique has been widely used to detect and partially characterize fragmentation events, contributing to a better understanding of the evolving debris environment [13,15].

In this study, we analyse two distinct space debris populations using monostatic beam-park observations

Proc. 9th European Conference on Space Debris, Bonn, Germany, 1–4 April 2025, published by the ESA Space Debris Office
Editors: S. Lemmens, T. Flohrer & F. Schmitz, (http://conference.sdo.esoc.esa.int, April 2025)

collected by the European Incoherent Scatter Scientific Association (EISCAT) [16] Ultra High Frequency (UHF) radar during two 24-h campaigns in July and August 2024. The first population is associated with a significant debris-generating event resulting from the fragmentation of the Long March 6A rocket [17], while the second corresponds to objects from the Starlink constellation [18]. To further validate our findings, a cross-comparison analysis is conducted, using radar detections alongside simulated detections obtained from the Program for Radar and Optical Observation Forecasting (PROOF) software [19] using the most recent available calibrated Meteoroid and Space Debris Terrestrial Environment Reference (MASTER) model population [19].

2 INSTRUMENTATION AND DATA

2.1 EISCAT UHF antenna

The UHF transmitter/receiver antenna, located in Tromsø (69.5°N, 19.2°E), was built in the late 1970s as part of a tri-static radar system for ionospheric observations. The antenna is a fully steerable Cassegrain-type dish with a 32m diameter main reflector and a nominal gain of 48.1 dB. The radar operates at a centre frequency of 933 MHz, with about 1 MHz of maximum usable transmit bandwidth. However, due to interference, its operating frequency has been adjusted several times during its operational lifetime. For example, the system operated at 927.6 MHz during the 2021 campaign, while the 2024 campaigns used a frequency of 927.2 MHz. Further details about the radar system can be found in [20].

2.2 The Hardtarget Library

The Hardtarget library [21] provides a set of tools for detecting and characterizing coherent echoes in raw (complex amplitude-level) radar data. At its core, the library implements routines for a Generalised Match Filter (GMF), which can be used to detect and determine the parameters of targets by integrating a phase model over multiple radar pulses.

The library is used for detections of meteors in atmospheric radar data, as well as for identifying RSOs, such as satellites and space debris, using ground-based radar systems.

2.3 The Resordan Library

The Resident Space Object Radar Data Analysis (RESORDAN) library [22] is designed for processing radar data related to space debris. It performs three key functions:

(i) Identifying detections in radar data by employing a clustering algorithm based on Signal-to-Noise Ratio (SNR) peaks.

(ii) Correlating detections with known objects using a catalogue of TLEs, as described in [20], and

(iii) Estimating the RCS values for each detection.

2.4 Radar Experiment

The radar experiment commonly used for observing space debris with the EISCAT radar systems is called LEO. This type of experiment uses a set of 64-bit codes with 30 µs bauds. The inter pulse period is 20 ms, allowing for coverage beyond 2500 km in slant range. A full cycle of the experiment is completed after transmitting and receiving a set of 128 individual 64-bit pulse sequences, which takes 2.56 s. For hard target detection, raw data (pre-integrated amplitude-level data) are also stored and processed offline.

In this study, beam-park observations were utilized. Since 2015, the primary pointing direction for these observations has been at an elevation of 75° and an azimuth of 90° (due east) [20]. However, in some cases, different pointing directions have been used based on the observation target. For instance, during the 22 August 2024, campaign, the objective was to detect debris from the Long March 6A event. To prioritize this observation, the antenna beam was adjusted to an elevation of 86° and an azimuth of 84°.

3 STARLINK

Fig. 1 shows the 24-h range (top panel) and range rate (bottom panel) detections as a function of time from the monos-tatic beam-park experiment conducted on 12–13 April 2021. Detections correlated with objects catalogued in Spacetrack [23] are marked with green circles, while uncorrelated detections are shown in black. The circle fill represents the Doppler shift, colour-coded according to the scale provided in the colour bar. Similarly, Fig. 2 illustrates the same parameters as Fig. 1 but for the 24-h campaign conducted on 4–5 July 2024.

A comparison of Fig. 1 and 2 reveals a persistent cluster of detections around 600 km in range, consistently observed throughout the experiment. The green circles in Fig. 2 indicate that these detections correspond to catalogued objects, which we identify as Starlink satellites. In all cases, the Doppler shift remains constant at approximately 2 km/s.

To analyse the temporal evolution of Starlink detections by the Tromsø radar, we examined all UHF LEO experiments conducted since 2015, focusing specifically on correlated detections. Fig. 3 presents this time evolution, distinguishing between all correlated objects (green) and Starlink satellites (magenta). Notably, Starlink objects are observed since the campaign of November 2021.

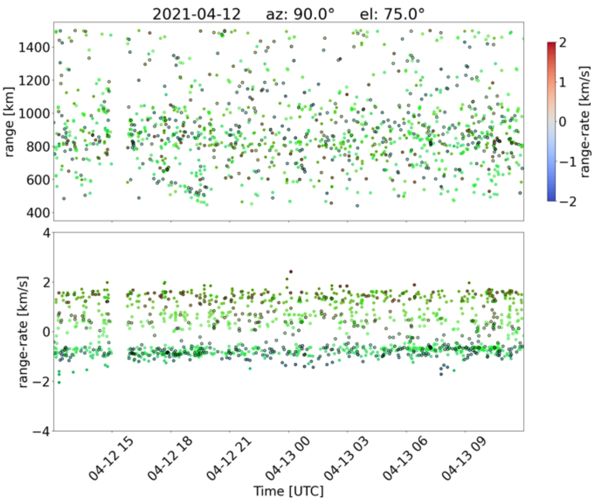

Figure 1. 24-h detections from the 12–13 April 2021 beam-park experiment. Correlated and uncorrelated detections are indicated with green and black circles, respectively. The circle fill is the Doppler shift, and it is colour-coded as indicated in the colour bar. The beam-park position is indicated in the title.

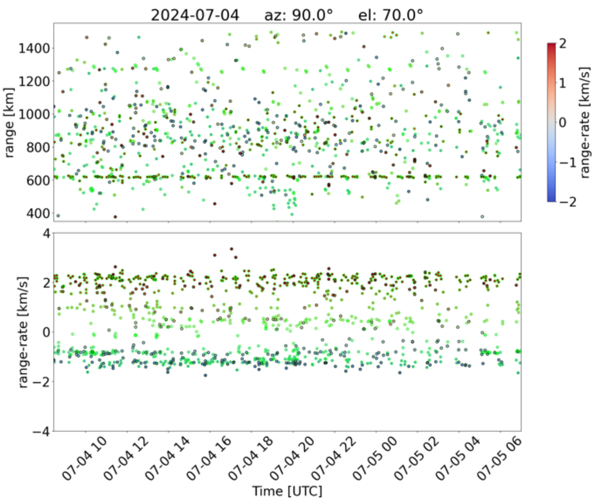

Figure 2. The same as Fig. 1 but for the 24-h campaign of 04–05 July 2024.

4 LONG MARCH 6A ROCKET

Fig. 4 shows the same parameters as Fig. 1 but for the 24-h campaign conducted on 22–23 July 2024. The Starlink constellation is clearly visible at approximately 600 km in range. Additionally, the figure reveals two distinct groups of uncorrelated objects (black circles): one appearing around 12 UTC and the other around midnight. Both clusters exhibit a Doppler shift close to 0 km/s.

To further investigate these detections, we computed the passes and orbit prediction of NORAD CAT ID 60397, corresponding to the CZ-6A R/B (rocket body), for the experiment's observation period. Our analysis indicates that this object could be observed at approximately 12 and 23 UTC with similar elevation angles. Consequently, the uncorrelated objects detected around 12 UTC and 23 UTC are most likely associated with debris from this rocket.

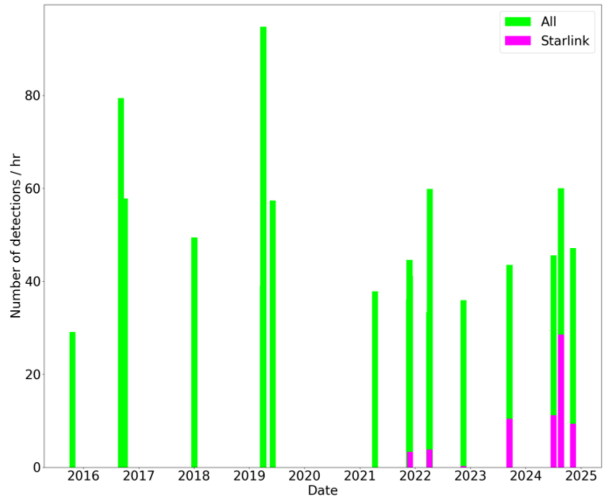

Figure 3. Temporal variation of detections after the correlation analysis. All detected objects are in green while Starlink objects are in magenta.

Figure 5 presents the correlated detections as a function of range rate and range for the 22–23 August 2024 campaign (red), alongside the simulated detections generated using the PROOF tool (grey). The overall distributions of range rate and range are shown in the top and right panels, respectively.

The figure reveals that the vertical variability in detection counts between the EISCAT and PROOF datasets is comparable. However, a notable discrepancy exists in the total detection count. The peak observed around 600 km correspond to Starlink satellites. Notably, the two datasets exhibit a distinct difference in detection range of approximately 50 km. On the other hand, the distribution of range rate between EISCAT and PROOF data shows less agreement, with most range rate detections being at least three times smaller in the simulations. While this remains a preliminary result, the observed discrepancies are intriguing.

5 DISCUSSION AND CONCLUSIONS

In this study, we utilized beam-park experiments to analyse two distinct populations of resident space objects.

Regarding Starlink, the deployment of the first satellites began in 2018. The earliest launches primarily consisted of satellites with an orbital inclination of 53°. In 2021, additional satellites were introduced with inclinations of approximately 97° and 70°. However, the number of satellites with these inclinations has varied over time. This temporal variability may help explain the observed reduction in Starlink detections toward the end of 2022.

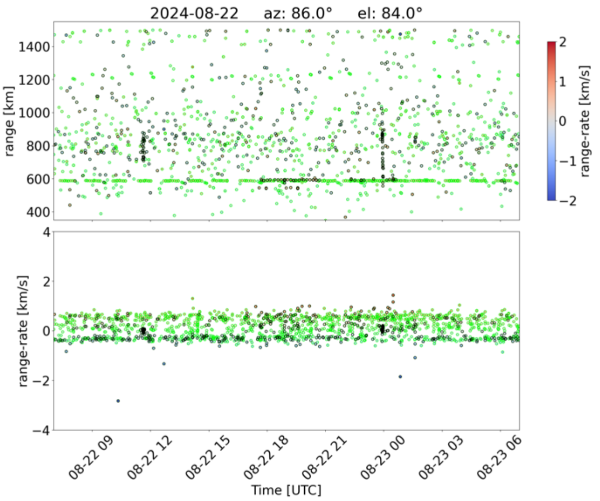

Figure 4. The same as Fig. 1 but for the 24-h campaign of 22–23 August 2024.

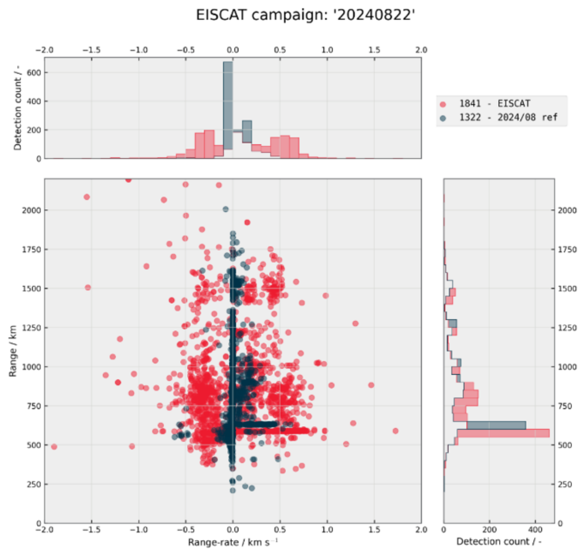

Figure 5. Radial range rate vs. range of simulated detections generated using the PROOF tool for the 22–23 August 2024 campaign. The overall range rate and range are displayed in the top- and right-side panels, respectively.

Regarding the Long March 6A rocket, the approach was to determine whether the detections are classified as uncorrelated. In other words, whether the detections did not match any known catalogued objects. Fig. 4 strongly suggests that the uncorrelated detections observed around 12 UTC are most likely associated with debris generated by the rocket breakup event.

A preliminary comparison between our results and those obtained using the PROOF model simulation shows differences in the number of detections, as well as in range and range rate parameters. Previous EISCAT beam-park data analyses have also exhibited discrepancies when compared with PROOF simulations [12]. The observed differences are not identical to those in past studies, this could be attributed to methodological variations between analyses. A more detailed examination of PROOF simulations, sensor modelling, and radar detection of weak signals could provide deeper insights into the discrepancies found in the present work.

Additionally, our current analysis is optimized to detect one target at a time. A potential improvement would be to expand the methodology to allow for increased detection rates per unit time. Finally, since the EISCAT database also contains beam-park experiment data from the EISCAT Svalbard Radar (ESR), we plan to extend our analysis to include these datasets in future work.

6 ACKNOWLEDGMENTS

We gratefully acknowledge the EISCAT staff for their assistance during the experiments and in preparation of data for further analysis. EISCAT was until 1 January 2025 an international association supported by research organizations in China (CRIPR), Finland (SA), Japan (NIPR and ISEE), Norway (NFR), Sweden (VR), and the United Kingdom (UKRI). On 1 January 2025 the association was transferred into a Swedish aktiebolag (AB). The new company, *EISCAT AB*, is owned by Sweden, Norway and Finland. This work was supported by the European Space Agency (ESA) Space Debris Office, under cooperative agreement ESA Contract No. 4000140805/23/D/KS.

7 REFERENCES

1. ESA (2025). Earth online. URL https://earth.esa.int/eogateway/missions/envisat (Accessed 22 March 2025).

2. Johnson, N., Krisko, P., Liou, J.-C., et al. (2001). NASA's new breakup model of evolve 4.0. *Adv. Space Res.*, 28(9), pp. 1377-1384, doi: 10.1016/S0273-1177(01)00423-9.

3. Braun, V., Lemmens, S., Reihs, B., et al. (2017). Analysis Of Breakup Events. *Proc. 7th European Conference on Space Debris*, ESA Space Debris Office, Darmstadt, Germany, pp. 13.

4. ESA (2025). About space debris. URL https://www.esa.int/Space_Safety/Space_Debris/About_space_debris (Accessed 22 March 2025).

5. Kessler, D.J., Cour-Palais, B.G. (1978). Collision frequency of artificial satellites: The creation of a debris belt. *J. Geophys. Res. Space Phys.*, 83(A6), pp. 2637-2646.

6. Liou, J.C., Anilkumar, A.K., Bastida Virgili, B., et al. (2013). Stability of the future LEO environment-an IADC comparison study. Ouwehand L. (Ed.), *6th European Conference on Space Debris*, ESA special publication, 723, pp. 2.

7. Rossi, A., Anselmo, L., Cordelli, A., et al. (1998). Modelling the evolution of the space debris population. *Planet. Space Sci.*, 46(11–12), pp. 1583-1596.

8. Rossi, A., Anselmo, L., Pardini, C., et al. (2009). The New Space Debris Mitigation (SDM 4.0) Long Term Evolution Code. *Proc. 5th European Conference on Space Debris*, ESA Space Debris Office, Darmstadt, Germany, pp. 8.

9. Lips, T., Fritsche, B. (2005). A comparison of commonly used re-entry analysis tools. *Acta Astronaut.*, 57(2–8), pp. 312-323, doi: 10.1016/j.actaastro.2005.03.010.

10. Klinkrad, H. (2006). Space Debris: Models and Risk Analysis. *Springer Science & Business Media*.

11. Markkanen, J., Lehtinen, M., Landgraf, M. (2005). Real-time space debris monitoring with EISCAT. *Adv. Space Res.*, 35(7), pp. 1197-1209, 10.1016/j.asr.2005.03.038.

12. Muntoni, G., Montisci, G., Pisanu, T., et al. (2021). Crowded Space: A Review on Radar Measurements for Space Debris Monitoring and Tracking. *Appl. Sci.*, 11(4), pp. 1364, 10.3390/app11041364.

13. Vierinen, J., Markkanen, J., Krag, H. (2009). High power large aperture radar observations of the Iridium-COSMOS collision. *Proc. 5th European Conference on Space Debris*, ESA Space Debris Office, Darmstadt, Germany, pp. 10.

14. Vierinen, J., Kastinen, D., Markkanen, J., et al. (2019). 2018 Beam-park observations of space debris with the EISCAT radars. *Proc. 1st NEO and Debris Detection Conference*, ESA Space Safety Programme Office, Darmstadt, Germany, 1(1), pp. 10.

15. Stansbery G. (2001). Preliminary results from the US participation in the 2000 Beam Park Experiment. *European Space Agency-Publications-ESA SP*, European Space Agency, 473, pp. 49-52.

16. ISCAT AB (2025). EISCAT AB. URL: https://eiscat.se (Accessed 22 March 2025)

17. Jones, A. (2024). China's Long March 6A rocket appears to have an orbital debris problem. *SpaceNews*. URL: https://spacenews.com/chinas-long-march-6a-rocket-appears-to-have-an-orbital-debris-problem/ (Accessed 22 March 2025).

18. Sesnic, T. (2022). Starlink Group 4-5 | Falcon 9 Block 5. *Everyday Astronaut*. URL: https://everydayastronaut.com/starlink-group-4-5-falcon-9-block-5-2/ (Accessed 22 March 2025).

19. ESA (2025). Space Debris User Portal. URL: https://sdup.esoc.esa.int (Accessed 22 March 2025)

20. Kastinen, D., Vierinen, J., Grydeland, T., et al. (2023). Using radar beam-parks to characterize the Kosmos-1408 fragmentation event. *Acta Astronautica*, 202, pp. 341-359.

21. Kastinen, D. (2025). Hardtarget. URL: https://github.com/danielk333/hardtarget (Accessed 22 March 2025)

22. Kastinen, D. (2025). Resordan. URL: https://github.com/danielk333/resordan/ (Accessed 22 March 2025)

23. Space-track (2025). Space-track. URL: https://www.space-track.org (Accessed 22 March 2025)